Desalination and Water Treatment
www.deswater.com

doi: 10.5004/dwt.2019.23578

144 (2019) 39–44
March

Polyamide hollow fiber composite nanofiltration membrane containing mesoporous silica intermediate layer

Yao Shi, Xinyu Zhao, Yining Sun, Yingbo Chen*, Hong Chen, Dongqing Liu

School of Materials Science and Engineering, State Key Laboratory of Separation Membranes and Membrane Processes, Tianjin Polytechnic University, Tianjin 300387, China

Received 7 August 2017; Accepted 6 May 2018

ABSTRACT

The conventional thin film composite nanofiltration membranes are composed of ultrafiltration support membrane and polyamide (PA) functional layer. It is required that the support membrane has suitable pore size, smooth surface, and compatibility with the PA functional layer to guarantee high performance of the composite nanofiltration membrane. In this study, a mesoporous silica intermediate layer was synthesized on the hollow fiber membrane to modify the support membrane for better composite membranes. The mesoporous silica layer was synthesized by hydrolysis of tetra orthosilicate with cetyltrimethylammonium bromide as template under acid aqueous solution. After removal, the template using ethanol/HCl solution, the modified support membranes were immersed in piperazine aqueous solution and trimesoyl chloride-hexane solution continuously for interfacial polymerization of PA on the silica layer. The composite membranes containing mesoporous silica were characterized by using scanning electron microscope, Fourier transform infrared spectroscopy, and water contact angle measurement. The performance of the composite membrane was discussed with regard to the effects of mesoporous silica layer, reaction time, and processing order. It was noticed that the intermediate mesoporous silica layer has positive effect on the performance of the composite membrane, including increasing salt rejection and increasing interfacial compatibility. The use of intermediate layer is a promising strategy to enhance the performance of composite membranes and extend the support membrane option.

Keywords: Nanofiltration; Mesoporous silica; Intermediate layer; Interfacial polymerization

1. Introduction

Nanofiltration membrane, with a pore size of about 1 nm, is a new type of functional semipermeable membrane which is between the ultrafiltration membrane and the reverse osmosis membrane. It has a low operating pressure and a high rejection characteristic for organic matters with small molecular weight. It also has the characteristics of different selectivity for monovalent and divalent ions [1]. Nanofiltration technology is a new type of pressure-driven membrane process developed to meet the needs of industrial softened water (removal of ions) and to reduce costs (reduce operating pressure), belonging to pressure-driven membrane separation technology. The preparation methods of nanofiltration membranes are mainly coating method, plasma polymerization method, and interfacial polymerization method. The interfacial polymerization on the support layer is the most effective method for the preparation of the nanofiltration composite membrane in the world [2]. It is also the largest variety and the largest yield method for production of nanofiltration membrane [3,4]. In a special operating environment, such as the filtrate containing a special solvent or high filtrate temperature, the physical and chemical stabilities of such nanofiltration membrane may be inadequate. Support membranes with strong physical and

---

* Corresponding author.

chemical stabilities, such as chemical inert organic materials, metals, or ceramics, can be a good solution to this point. However, the pore size of these supports is usually mismatched with the functional layer of the composite membrane, and the compatibility between the support and the functional layer is also relatively poor. This situation greatly limits these materials with extremely excellent comprehensive performance to become the support of the nanofiltration composite membrane. It has become an urgent need to prepare an intermediate functional layer connecting the support and the surface functional layer with a suitable membrane pore size and a strong compatibility, so as to prepare nanofiltration membranes with different types of supports to meet the membrane separation in special cases.

TiO_2 nanoparticles (NPs) have attracted much attention in the surface modification of polymer membranes due to their excellent hydrophilicity. For example, Pi et al. fabricated TiO_2-modified microfiltration membranes by using a polydopamine/polyetherimide intermediate layer via a sol–gel process. TiO_2 NPs can effectively improve the surface wettability and water permeation property of the hydrophobic membranes [5]. In addition, Wang et al. prepared a kind of layer-by-layer structured polyamide (PA)/ZIF-8 (zeolitic imidazolate framework-8) nanocomposite membrane and achieved a 60% higher water flux than pristine PA membrane [6]. Yin et al. prepared a thin film nanocomposite membrane containing graphene oxide (GO) nanosheets by the in-situ interfacial polymerization process. Results indicated that the GO nanosheets were dispersed well in the PA layer and their incorporation improved membrane performance [7].

In this paper, in order to prepare a novel thin film composite membrane containing SiO_2, a mesoporous silica layer was synthesized by hydrolysis of ethyl orthosilicate (TEOS) with cetyltrimethylammonium bromide (CTAB) as template under acid aqueous solution. After removal of the template using ethanol/HCl solution, the modified support membranes were immersed in piperazine (PIP) aqueous solution and trimesoyl chloride (TMC)-hexane solution continuously for interfacial polymerization of PA on the silica layer. The composite membranes containing mesoporous silica were characterized by using scanning electron microscopy (SEM), Fourier transform infrared spectrometer (FTIR), and water contact angle measurement. The performance of the composite membrane was discussed with regard to the effects of mesoporous silica layer, reaction time, and processing order.

2. Experimental part

2.1. Materials

Polyvinylidene fluoride hollow fiber membrane (PVDF, with inside diameter 1,000 μm and outer diameter 600 μm) was purchased from Tianjin Motimo Membrane Technology Ltd. Co., Tianjin, China; CTAB; TEOS, and PIP were purchased from Tianjin Kemio Chemical Reagent Ltd. Co., Tianjin, China; epoxy resin (modified acrylate cementing compound) was purchased from Liaoning Fushun GOOD BROTHERS New Material Ltd. Co., Liaoning, China; and TMC and *n*-hexane were purchased from Tianjin Fengchuan Chemical Reagent Ltd. Co., Tianjin, China.

2.2. Preparation of PVDF/mesoporous silica/PA composite hollow fiber nanofiltration membrane

Each PVDF hollow fiber ultrafiltration membrane (20 cm) was sealed at both ends with epoxy resin and then dried in air for 6 h. The reaction solution was prepared by adding 9.73 g CTAB, 70 g deionized water, and 352 μL hydrochloric acid solution (1 mol L^{-1}) into a beaker, and then it was stirred at a constant temperature of 40°C for 20 min in a water bath followed by addition of 13 g TEOS and stirred at room temperature for 30 min. The fibers were completely immersed in the solution for 5 h and dried at room temperature for 20 min. The fibers were transferred into another tube in which 90 mL of 0.05 mol/LHCl alcohol solution were added for extraction for 24 h to remove the template (CTAB) in order to prepare PVDF/mesoporous silica hollow fiber composite membrane [8,9].

The PVDF/mesoporous silica hollow fiber composite membrane was put in aqueous phase (2 w/v% PIP) for 5 min. Excess aqueous phase was removed by passing the hollow fiber membrane through filter paper with a pore smaller than the external diameter of the hollow fiber membrane. The hollow fiber membrane was then put into oil phase (0.15 w/v% TMC/*n*-hexane) for 5 min followed by drying at 70°C for 5 min. PIP and TMC were interfacial polymerized on the outer surface of PVDF/mesoporous silica composite film to form PA dense film layer. The PVDF/mesoporous silica/PA nanofiltration composite membrane was prepared as shown in Fig. 1. As a comparison, the composite nanofiltration membrane prepared with PVDF as the support was prepared directly on the PVDF support membrane using the similar method as above.

2.3. Characterization of hollow fiber composite nanofiltration membrane

SEM was conducted by using field emission SEM (Japan Hitachi FESEM S-4800, Hitachi, Japan). The samples were immersed in liquid nitrogen to obtain a smooth cross section and sprayed with gold before the SEM observation. Infrared spectroscopy of the hollow fiber composite nanofiltration membrane was recorded by using FTIR (Germany Bruker Company type Tensor37, Germany) with scanning in the range of 400–4,000 cm^{-1}. The hydrophilicity of hollow fiber composite nanofiltration membrane was tested by contact angle measurement. The membrane pasted on a glass pane was placed on the platform of the contact angle measurement machine. Five microliters water was dropped on the surface of the membrane for testing the contact angle in sessile drop method (Germany KRUSSA Company Type DSA100, Germany). It was tested for 5 times per sample to calculate an average value.

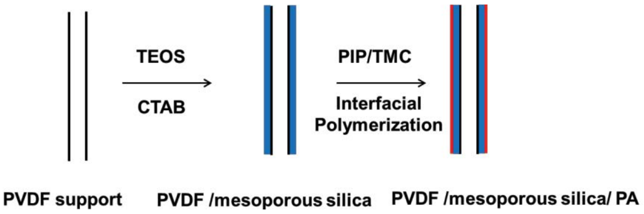

Fig. 1. The illustration of the preparation of composite hollow fiber nanofiltration membrane.

2.4. Performance of hollow fiber composite nanofiltration membrane

Water flux of the membranes was tested by a homemade membrane evaluation device (Fig. 2) [10] at 0.4 MPa. Four hollow fiber nanofiltration membranes were assembled in a membrane module for testing. Water flux of the membrane was calculated by Eq. (1):

$$J = \frac{V}{S \times t} \tag{1}$$

where J stands for water flux (L m^{-2} h^{-1}), V stands for penetrated water volume of membrane in certain time (L), S stands for the active area of membrane (m^2), t stands for performance period (h).

Rejection (R) of the membrane was calculated using Eq. (2):

$$R = \frac{1 - C_P}{C} \times 100\% \tag{2}$$

where C_P is the concentration of permeate and C is the concentration of the feed solution.

The concentration of permeate and feed was measured by conductivity. The feed is 1 g L^{-1} Na_2SO_4 aqueous solution. It was tested for 3 times per sample to calculate an average value of flux or rejection.

3. Results and discussion

3.1. SEM images of hollow fiber composite nanofiltration membrane

As shown in Fig. 3(a), a lot of defects on the outer surface of the support membrane resulted in high water flux and a small rejection rate. Fig. 3(b) shows the surface of the mesoporous silica layer. The defects of the PVDF support disappeared due to the cover of the mesoporous silica layer. Figs. 3(c) and (d) show the surface of PA layer directly interfacial polymerized on the PVDF support membrane. Fig. 3(c) shows the treatment with oil phase before the aqueous phase and Fig. 3(D) the treatment with aqueous phase before the oil phase. We can see the obvious PA layer, but there are still some pores on the surface, resulting in the phenomenon of high flux and low salt retention. The surface of the membrane treated with the aqueous phase first (Fig. 3(c)) shows a nodular structure resulting from intense interface polymerization. On the other hand, the surface shown in Fig. 3(d) is relatively smooth, and the degree of reaction is low because the supporting layer has poor wettability to the oil phase. Fig. 3(e) shows the surface of the PVDF/mesoporous silica/PA composite nanofiltration membrane treated with aqueous phase before the oil phase. Because of the increased interfacial compatibility of the silica layer, the interfacial polymerization reaction was slow and sufficient. So the membrane surface is very regular, and the resulting layer is uniform and homogeneous, which greatly improves the performance of the composite membrane. Fig. 3(f) shows the surface of the PVDF/mesoporous silica/PA composite nanofiltration membrane treated with oil phase before the aqueous phase. The degree of interfacial polymerization also was low because the silica layer is oleophobic. So there are many pores on the surface, resulting in high flux and low retention.

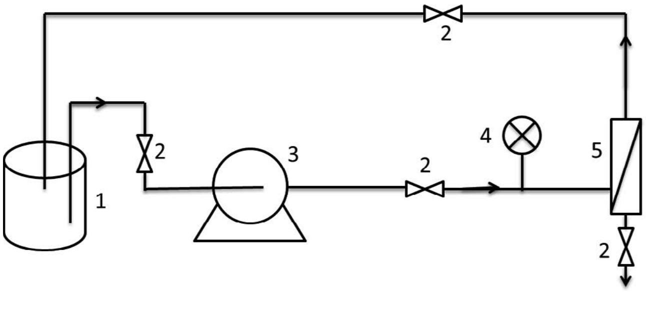

Fig. 2. Scheme of the setup for membrane performance evaluation. 1. Store tank; 2. Throttle; 3. Pump; 4. Pressure gauge; 5. Membrane module.

Figs. 4(a) and (b) are SEM images of the PVDF support membrane. Fig. 4(c) shows the PVDF/SiO_2 composite membrane with in situ reaction, in which we can see the obvious stratification. Fig. 4(d) (aqueous phase-oil phase) and Fig. 4(e) (oil phase-aqueous phase) show polymerization carried out directly in the support membrane surface. We can see the distribution of uneven and incomplete PA layer structure. Fig. 4(f) is the PVDF/SiO_2/composite nanofiltration membrane (aqueous phase-oil phase), in which we can see that it has a three-layer structure. The inner layer is PVDF support, the middle is mesoporous silica, and the outer layer is dense PA layer. Fig. 4(g) is PVDF/SiO_2/composite nanofiltration membrane (oil phase-aqueous phase). It clearly shows the porous PA coating on the surface. The above results are consistent with SEM surface images and their reaction mechanism.

3.2. Analysis of FTIR characterization

Fig. 5 is the FTIR spectra of PVDF, PVDF/SiO_2, and PVDF/SiO_2/PA membranes. The weak infrared absorption at 3,418 cm^{-1} corresponds to the stretching vibration absorption peak of the N–H or O–H end groups of the trimellamide macromolecules. The strong absorption at 1,626 cm^{-1} is the absorption peak of the carbon group in the amide. The peak at 1,730 cm^{-1} is the acid chloride characteristic absorption peak. The absorption peaks at 1,019 and 1,033 cm^{-1} are Si–O–Si asymmetric stretching vibration peaks. The absorption peak at 1,019 cm^{-1} is summarized for three reasons: (1) Si–O–Si stretching vibration, (2) Si–Si stretching vibration, and (3) tetrahedral symmetrical telescope, which constitutes a typical characteristic absorption peak of SiO_2, indicating that the composition of the sample is SiO_2 and the PA layer was successfully prepared.

3.3. The effect of mesoporous silica

PVDF/PA composite film and PVDF/SiO_2/PA composite film were prepared under the same experimental conditions (2% PIP aqueous phase solution, 0.15% TMC oil phase solution) and tested under the same conditions, the performance of the composite membranes are shown in Table 1. Under the above preparation conditions, water flux of the PVDF/SiO_2 composite membrane was 85.71 L m^{-2} h^{-1} and the 1 g L^{-1} Na_2SO_4 rejection rate was 24.6%. However, the flux of

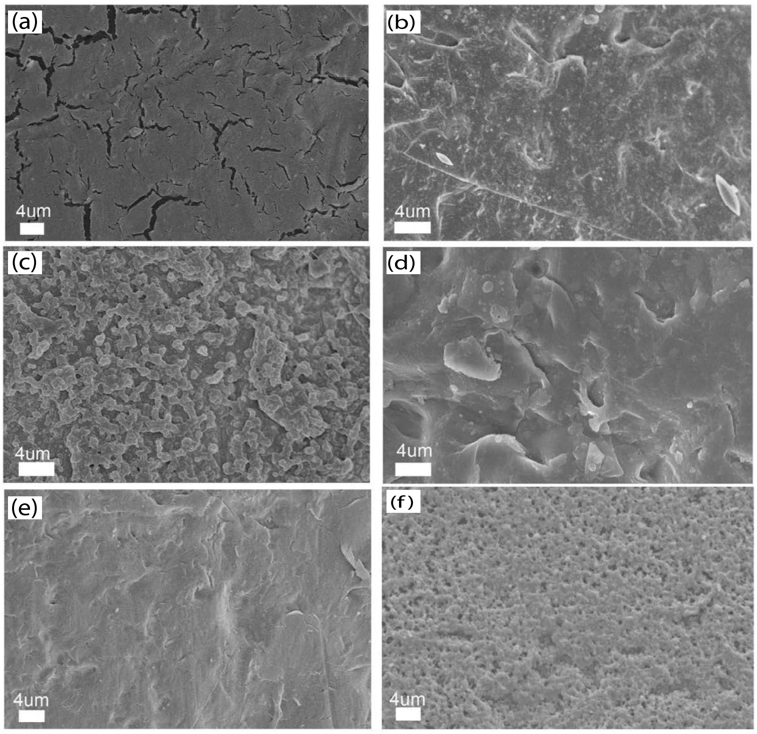

Fig. 3. SEM surface images of PVDF membrane (a), PVDF/SiO$_2$ membrane (b), PVDF/PA (aqueous phase-oil phase) membrane (c), PVDF/PA (oil phase-aqueous phase) membrane (d), PVDF/SiO$_2$/PA (aqueous phase-oil phase) membrane (e), and PVDF/SiO$_2$/PA (oil phase-aqueous phase) membrane (f).

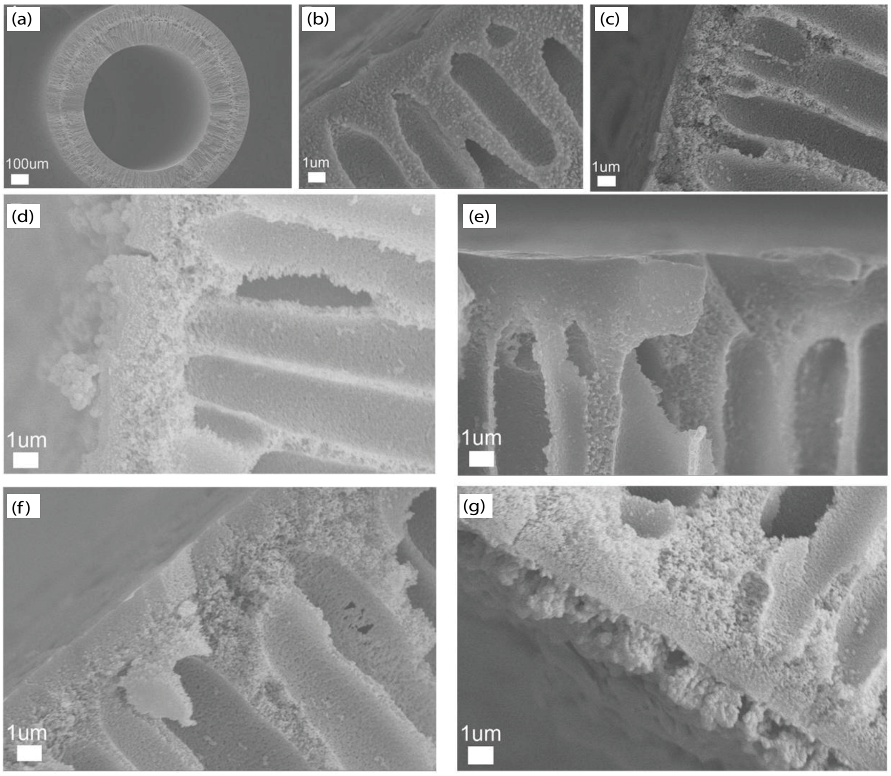

Fig. 4. SEM cross-section images of PVDF membrane (a, b), PVDF/SiO$_2$ membrane (c), PVDF/PA (aqueous phase-oil phase) membrane (d), PVDF/PA (oil phase-aqueous phase) membrane (e), PVDF/SiO$_2$/PA (aqueous phase-oil phase) membrane (f), PVDF/SiO$_2$/PA (oil phase-aqueous phase) membrane (g).

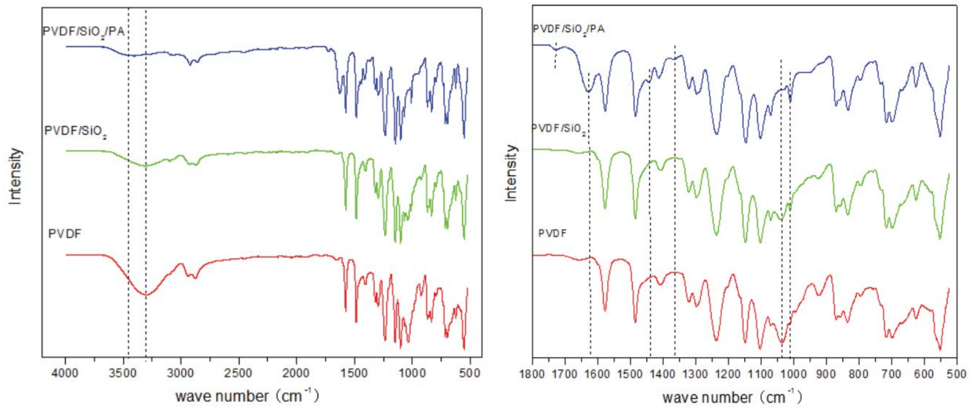

Fig. 5. FTIR spectra of PVDF, PVDF/SiO$_2$, and PVDF/SiO$_2$/PA membranes.

Table 1
Water flux, Na_2SO_4 rejection, and water contact angle of PVDF support membrane, PVDF/SiO$_2$ membrane, PVDF/PA membrane, and PVDF/SiO$_2$/PA membrane

Membranous type	Water flux, L m^{-2} h^{-1}	Na_2SO_4 rejection, %	Contact angle (°)
PVDF	181.58	3.03	84.5 ± 11.3
PVDF/SiO$_2$	16.75	7.03	64.3 ± 12.6
PVDF/PA (A-O)*	85.71	24.60	25.3 ± 5.7
PVDF/PA (O-A)	126.25	22.37	75.9 ± 6.4
PVDF/SiO$_2$/PA (A-O)	3.57	87.80	20.2 ± 5.2
PVDF/SiO$_2$/PA (O-A)	7.14	38.30	56.6 ± 8.3

*A-O means the hollow fiber immersing in aqueous phase first and then in oil phase; O-A means the hollow fiber immersing in oil phase first and then in aqueous phase.

PVDF/SiO$_2$/PA composite membrane was 3.57 L m^{-2} h^{-1}, and the rejection rate was 87.8%. Compared with the composite film without the middle layer, the flux of the composite membrane with the mesoporous silica functional layer as the intermediate layer decreased significantly, while the rejection rate increased greatly. PVDF hollow fiber membrane support is ultrafiltration membrane, so the membrane pore size is larger, but polymerized polypiperazine amide functional layer pore size is very small, resulting in poor compatibility between them. During the process of membrane operation, due to the large difference in membrane pore size between them, the water pressure may crush the functional layer, resulting in losing the role of the functional layer, so there is a high-flux and low-rejection experimental results, which are consistent with the SEM images. The pore size of the composite membrane with mesoporous silica functional layer as the intermediate layer ranged from the pore size of the support and the pore size of the polypiperazine amide membrane, which greatly solves the problem of compatibility.

The PVDF/SiO$_2$/PA composite film was prepared under the same experimental conditions (2% PIP aqueous solution, 0.15% TMC oil phase solution), and then the sequential treatment of the water phase and oil phase was changed to investigate the effect of the sequential treatment of the water and oil phases on the performance of the composite nanofiltration membrane. The water flux of the PVDF/SiO$_2$/PA (aqueous phase-oil phase) membrane was 3.57 L m^{-2} h^{-1}, and the rejection rate was 87.8%. On the other hand, the water flux of the PVDF/SiO$_2$/PA (oil phase-aqueous phase) membrane was 7.14 L m^{-2} h^{-1}, and the rejection rate was 38.3%. The PA layer formed by treating in the aqueous phase after the oil phase was relatively loose and not dense, leading to the phenomenon of high flux and low retention. This is because both the support layer and the silica layer are hydrophilic and have poor wettability to the oil phase, so the degree of reaction is low. The porous PA layer also can be clearly seen from the SEM images.

The contact angle of PVDF support membrane (84.5°) was large due to the hydrophobicity of PVDF. Because of the presence of silylates, the hydrophilicity of the PVDF/SiO$_2$ composite film was improved to a certain extent, with a contact angle of 64.3°. The hydrophilicity of the PVDF/SiO$_2$/PA (aqueous phase-oil phase) membrane with a contact angle of 20.2° was obviously improved after interfacial polymerization, due to the hydrophilicity of the PA layer. In addition, more acyl chloride residues remain on the surface of the membrane after the interfacial polymerization, which can be hydrolyzed to carboxyl. Therefore, the hydrophilicity of the membrane is improved, while the PVDF/SiO$_2$/PA (oil phase-aqueous phase) membrane had a contact angle of 56.61°.

3.4. The effect of the treatment time of the aqueous phase

PVDF/SiO$_2$/PA composite hollow fiber nanofiltration membranes prepared at different aqueous phase immersion times (1, 3, 5, 7, and 9 min) were used to measure the water flux and the retention of 1 g L^{-1} Na_2SO_4 aqueous solution. When aqueous phase time was 1 min, the water flux was 5.36 L m^{-2} h^{-1} and the rejection rate was 62.5% (Fig. 6). The water flux of composite membrane decreased first and then increased with the increase of time, while the rejection rate increased first and then decreased. The flux was 3.57 L m^{-2} h^{-1} and the rejection rate was 87.8%, which reached a maximum at 5 min. Thereafter, as the contact time continued to rise, the flux of the composite nanofiltration membrane increased gradually and the rejection rate decreased rapidly. The reason for this phenomenon is that when the aqueous phase time was short, the microporous adsorption water phase did

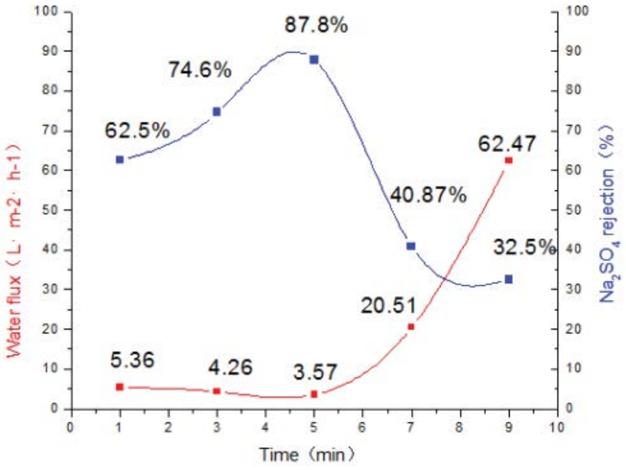

Fig. 6. The water flux and rejection rate of different times of the aqueous phase.

not reach the saturation state, so the interface polymerization could not produce uniform and form dense PA layer. In addition, because PIP aqueous solution was alkaline, the first layer of mesoporous silica layer was destroyed and then the overall structure of the film was damaged with the increase in aqueous phase time, resulting in increased flux and decreased rejection.

4. Conclusion

The PVDF/SiO_2/PA composite hollow fiber nanofiltration membrane was prepared by interfacial polymerization of PA on PVDF hollow fiber support membrane. SEM and FTIR analyses proved that the mesoporous silica layer was well attached to the surface of the support membrane. When aqueous phase time was 1 min, the flux was 3.57 L m^{-2} h^{-1} and the rejection rate was 87.8%. It is proved that it is feasible to connect the support membrane and the surface separation layer with the intermediate functional mesoporous silica layer. The composite nanofiltration membrane prepared by interface polymerization can be more widely used with varied support membranes through a mesoporous silica as the intermediate layer. However, the flux of the composite nanofiltration membrane was relatively low due to the resistance of the silica layer. Larger pore size of the mesoporous silica layer can be used to enhance the flux for further research.

Acknowledgements

The authors acknowledge the financial support from the Science and Technology Plans of Tianjin (No. 16YFZCSF00330, 16PTSYJC00100) and Tianjin Student's Platform for Innovation and Entrepreneurship Training Program (201610058083).

References

[1] X. Liang, J. Li, Z. Chen, Development of novel materials for nanofiltration membranes, J. Filtr. Sep., 16 (2006) 18–21.
[2] Y. Mansourpanah, S.S. Madaeni, A. Rahimpour, Fabrication and development of interfacial polymerized thin-film composite nanofiltration membrane using different surfactants in organic phase: study of morphology and performance, J. Membr. Sci., 343 (2009) 212–228.
[3] J.M. Peng, Y.L. Su, W.J. Chen, X.T. Zhao, Polyamide nanofiltration membrane with high separation performance prepared by EDC/NHS mediated interfacial polymerization, J. Membr. Sci., 427 (2013) 92–100.
[4] A. Rahimpour, M. Jahanshahi, N. Mortazavian, Preparation and characterization of asymmetric polyethersulfone and thin film composite polyamide nanofiltration membranes for water softening, Appl. Surf. Sci., 256 (2010) 1657–1663.
[5] J.-K. Pi, H.-C. Yang, L.-S. Wan, J. Wu, Z.-K. Xu, Polypropylene microfiltration membranes modified with TiO_2, nanoparticles for surface wettability and antifouling property, J. Membr. Sci., 500 (2016) 8–15.
[6] L. Wang, M. Fang, J. Liu, J. He, J. Li, J. Lei, Layer-by-layer fabrication of high-performance polyamide/Zif-8 nanocomposite membrane for nanofiltration applications, ACS Appl. Mater. Interfaces, 7 (2015) 24082–24093.
[7] J. Yin, G. Zhu, B. Deng, Graphene oxide (GO) enhanced polyamide (PA) thin-film nanocomposite (TFN) membrane for water purification, Desalination, 379 (2016) 93–101.
[8] F. Chen, X. Li, Z. Li, Y.K. Shao, Influence of HCl content on the morphology of silica, Bull. Chin. Ceram. Soc., 31 (2012) 1001–1625.
[9] Q. Li, Z.K. Li, H. Yu, X.H. Pan, X.L. Wang, Y.H. Wang, J. Song, Effects of ordered mesoporous silica on the performances of composite nanofiltration membrane, Desalination, 327 (2013) 24–31.
[10] C.Y. Liu, J.Q. Wang, B.M. Li, Preparation and characterization of ordered mesoporous silica membrane, J. Non-Cryst. Solids, 351 (2005) 409–412.